https://doi.org/10.5194/ar-2024-39
Preprint. Discussion started: 13 December 2024

Impact of Sampling Frequency on Low-Cost PM Sensor Performance

Gulshan Kumar[1], Prasannaa Kumar D.[1], Saran Raj[1], Jay Dhariwal[1,+], and Seshan Srirangarajan[2,*]

[1]Department of Design, Indian Institute of Technology Delhi, New Delhi 110016, India
[2]Department of Electrical Engineering, Indian Institute of Technology Delhi, New Delhi 110016, India
[+]jay@design.iitd.ac.in
[*]seshan@ee.iitd.ac.in

Abstract. Low-cost sensors for particulate matter (PM) monitoring have gained popularity due to their affordability, compact size, and low power requirements. These sensors typically offer the capability to collect data at sampling rates that can be adjusted according to the application. However, the effect of varying the sampling frequency on sensor performance has not been thoroughly examined. This study explores how variations in sampling frequency influence the performance of low-cost PM sensors and identifies some possible use cases for different sampling rates. During this study conducted over a one month period, data from five SPS30 sensors was collected at 15 second intervals and then aggregated into 5, 10, 15, 30, and 60 minutes intervals. During the study, hourly $PM_{2.5}$ levels ranged from 117 μg/m^3 to 303.3 μg/m^3, with significant diurnal variations, influenced by temperature and humidity. It was found that changes in sampling frequency had minimal impact on sensor performance, as evidenced by comparable linearity and error metrics across different sampling intervals. However, the study also revealed that short-lived plume events could be missed at lower sampling frequencies. This suggests that for monitoring gradual changes in $PM_{2.5}$ levels, higher sampling frequencies do not necessarily improve measurement accuracy, but are crucial for capturing transient events. This study underscores the importance of optimizing sampling frequency based on specific monitoring objectives and the need to balance power consumption with data resolution, particularly in remote or battery-based deployments.

1 Introduction

Low-cost sensors (LCS) for particulate matter (PM) monitoring have generated significant attention within the scientific community due to their affordability and performance (Liu et al., 2020; Giordano et al., 2021). Their compact design makes them well-suited for portable applications, while their affordability allows for widespread deployment, facilitating the establishment of spatio-temporal networks for high resolution pollution data (Jiao et al., 2016; Zheng et al., 2019; Yi et al., 2015). Moreover, their low power consumption makes them suitable for standalone use, including scenarios where battery or solar power can be utilized (Lung et al., 2020; Das et al., 2022; Gulia et al., 2020; McKercher et al., 2017). These sensors serve diverse purposes, ranging from personal exposure monitoring (Helbig et al., 2021; Xi et al., 2022) to the creation of extensive data collection networks for ambient air pollution monitoring (Jain et al., 2021; Koehler and Peters, 2015). Additionally, the United

https://doi.org/10.5194/ar-2024-39
Preprint. Discussion started: 13 December 2024

States Environmental Protection Agency's (USEPA) acceptance of LCS for non-regulatory applications further underscores their utility (Duvall et al., 2021; Malings, 2024).

LCS have the capability to generate data at high frequency (~ 1 sample/s) (Sensirion, 2024; Plantower, 2024; Honeywell, 2024), and are typically calibrated against optical particle counters (OPC) using known particles such as monodisperse polystyrene latex (PSL) beads for lab testing (Kaur and Kelly, 2023). The calibration involves averaging the high-frequency LCS data to match the sampling frequency of reference monitors, followed by assessment against the USEPA-recommended metrics (Duvall et al., 2021).

While it is widely assumed that higher frequency LCS data collection aligns more closely with the results obtained from reference sensors, configuring LCS to operate at high sampling rates leads to increased power consumption. This issue is particularly critical in remote deployments where a direct power supply may not be available and it can rapidly drain battery reserves. Conversely, lowering the sampling frequency may lead to the loss of critical information and a weaker correlation with reference monitors. Despite the widespread deployment of LCS, there remains a significant gap in research regarding the optimal sampling frequency for accurate data collection. This lack of understanding makes it difficult to recommend a sampling rate that balances the need to achieve performance close to that of the reference monitor with the specific requirements of the application.

In the context of short-term exposure measurement, accurately capturing brief, high-intensity plume events such as diesel generator emissions (Fadel et al., 2022; Greim, 2019; Gilmore et al., 2006), vehicular emissions (Zhang and Batterman, 2013; Lipfert and Wyzga, 2008), cooking (Chu et al., 2021; Xiang et al., 2021; Sharma and Jain, 2019; Balakrishnan et al., 2004), or waste burning (Wiedinmyer et al., 2014; Kumari et al., 2019) is very important. These transient spikes in $PM_{2.5}$ levels can have a significant impact on daily air quality and are linked to adverse health effects, including airway inflammation and other complications (Salvi et al., 1999; Gong et al., 2003; Pope and Dockery, 2006). Although both short- and long-term exposures are associated with health risks, the methods to monitor them are different. Long-term exposure can often be monitored with lower frequency sampling, which is adequate to detect general pollution trends. However, accurately assessing short-term exposure requires high-frequency data to capture the plume events. In personal exposure monitoring, it is important to evaluate both the exposure level and the corresponding dose (Borghi et al., 2020, 2021). Low sampling frequencies may suffice for broad exposure assessments, but high-frequency data is necessary to accurately measure the dose. This highlights the need to optimize sampling strategies based on specific monitoring objectives, such as assessing overall exposure or capturing the dose during short-lived events.

This study, conducted over a period of one month, uses Sensirion SPS30 LCS collocated with a reference grade beta attenuation monitor (BAM). The data from LCS was recorded at 15 second intervals and subsequently aggregated over 5, 10, 15, 30, and 60 minutes intervals. To assess the impact of sampling frequency, parameters such as linearity and error were evaluated for different sampling frequencies. In this work, the measurements and analysis were designed to address the following questions: (1) Do the different sampling intervals have an effect on sensor performance compared to BAM? (2) How does sampling frequency affect the identification of short-lived local pollution events?

https://doi.org/10.5194/ar-2024-39
Preprint. Discussion started: 13 December 2024

2 Methods

2.1 Sensirion SPS30 $PM_{2.5}$ Sensor

SPS30 is a PM sensor from Sensirion and has been used in multiple low-cost monitors and well-evaluated for outdoor applications (Tryner et al., 2020; Roberts et al., 2022). Low-cost PM sensors estimate the PM mass concentration based on light scattering. SPS30 uses a 660 nm laser diode for light scattering (Sensirion, 2024). The sensor uses an auto-cleaning feature to maintain the airflow rate by cleaning the airflow path. The sensor also supports sleep mode for reducing power consumption when it is not actively sampling. The current drawn is as low as 50 μA during sleep mode (SPS). Based on the coefficient of determination (R^2), for outdoor $PM_{2.5}$ measurements, SPS30 is among the best-performing LCS (AQS). In this study, five Sensirion SPS30 sensors were utilized and will be referred to as S1-S5 in this article.

2.2 Sensor Cluster Design

A custom monitoring device was designed and developed for this study using five SPS30 LCS (refer Figure 1). In this device, SPS30 sensors communicate with the microcontroller (MCU) using the I^2C protocol. Each SPS30 sensor has a predetermined I^2C address, 0x69 (Sensirion, 2024). Since I^2C uses common lines and all five sensors have identical addresses, an I^2C multiplexer was used (I2C). A custom-designed printed circuit board (PCB) with inbuilt real-time clock (RTC), SD card connector, OLED display, and power management IC was used. ESP32 MCU was used for data acquisition from the sensors. The data was stored along with the timestamp on an SD card. A 12 second interval between sensor data acquisition was established to synchronize with the I^2C multiplexer. The data stored on the SD card can be accessed using the file transfer protocol (FTP) over a Wi-Fi client, with a magnetic reed switch facilitating the activation of the FTP protocol during data transfer. 3D-printed parts were used as sensor holders and to guide the airflow along the inlet and outlet paths. Each sensor's sampling inlet and outlet were isolated from the others using a 3D-printed part.

2.3 Reference Monitor BAM

The BAM-1020 from Met One Instruments served as the reference monitor. Operating on the beta-ray attenuation technique, this monitor is approved by the USEPA for regulatory purposes. The $PM_{2.5}$ data collected from the BAM is available at an hourly resolution. Additionally, temperature and humidity data from the BAM's ambient sensor were also recorded. Throughout the study, the BAM's error logs were regularly checked.

2.4 Site Description and Metereology

The experiment site was located inside the Indian Institute of Technology Delhi, New Delhi campus (28°32'37.5"N 77°11'31.1"E). The LCS cluster and BAM were kept within 0.5 m of each other on the roof of a single-storey building. Their inlet heights were set at 1 m from the roof surface, facilitating unobstructed airflow throughout the experiment. The experiment was conducted during the month of October 2023. During the experiment, ambient $PM_{2.5}$ exposure ranged from 11.7 $\mu g/m^3$ to 303.3 $\mu g/m^3$

https://doi.org/10.5194/ar-2024-39
Preprint. Discussion started: 13 December 2024

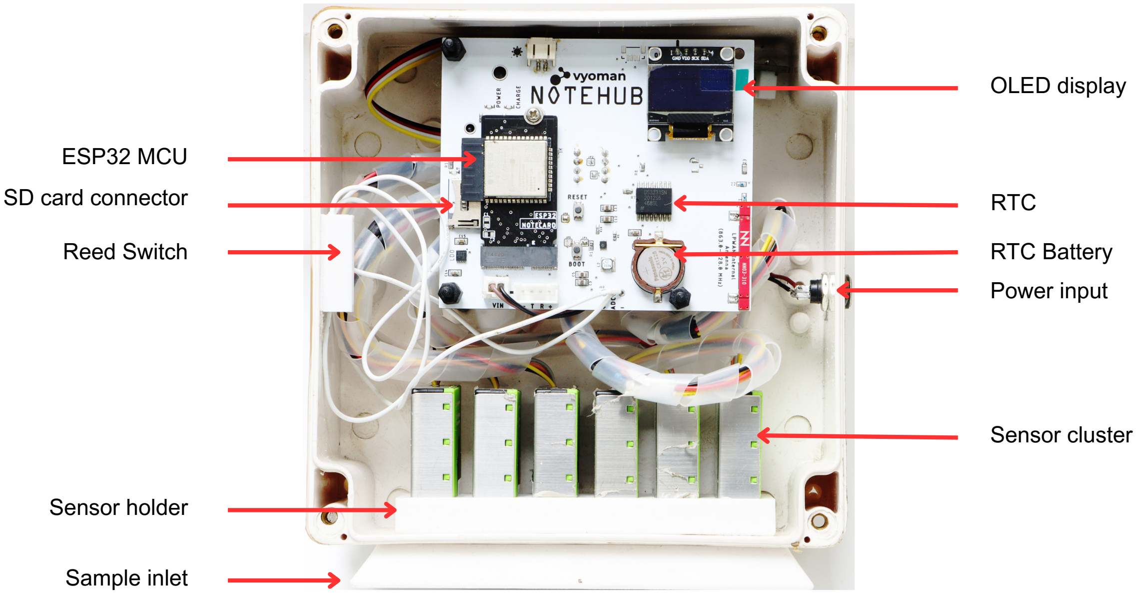

Figure 1. PM monitoring device design.

with an average exposure of 84.4 μg/m^3. In addition, the temperature ranged from 16.6 °C to 36.6 °C, with an average of 25.49 °C, and the relative humidity (RH) levels were between 27% and 93% with an average value of 65%. The recorded data is shown in Figure 2.

The experimental setup was strategically placed on the roof of a single-storey building (refer Figure 3) to ensure unrestricted airflow, with no nearby obstructions. Around the study site, a campus road is about 40 m away, while taller buildings which are 4-5 storeys high, are located about 60 m away. In addition, a backup diesel generator is located about 30 m away at the ground level.

Since October falls in the post-monsoon season in India, occasional rainy days were observed during the experiment, notably impacting temperature trends following the rainfall on 16th and 17th October, 2023. Figure 2 shows the variations in meteorological conditions and $PM_{2.5}$ levels during the study period, highlighting the dependence between the environmental factors and air quality. It is observed that $PM_{2.5}$ levels increase with rising humidity levels in the morning. As temperatures rise in the afternoon, the humidity levels decrease, leading to a drop in $PM_{2.5}$ concentrations (refer Figure 4). In the evening hours, as humidity levels rise again, $PM_{2.5}$ levels gradually increase. The peak $PM_{2.5}$ levels are observed around 8:00 am and can be attributed to increased vehicular emissions, while lowest $PM_{2.5}$ levels are observed in the afternoon due to higher temperature

https://doi.org/10.5194/ar-2024-39
Preprint. Discussion started: 13 December 2024

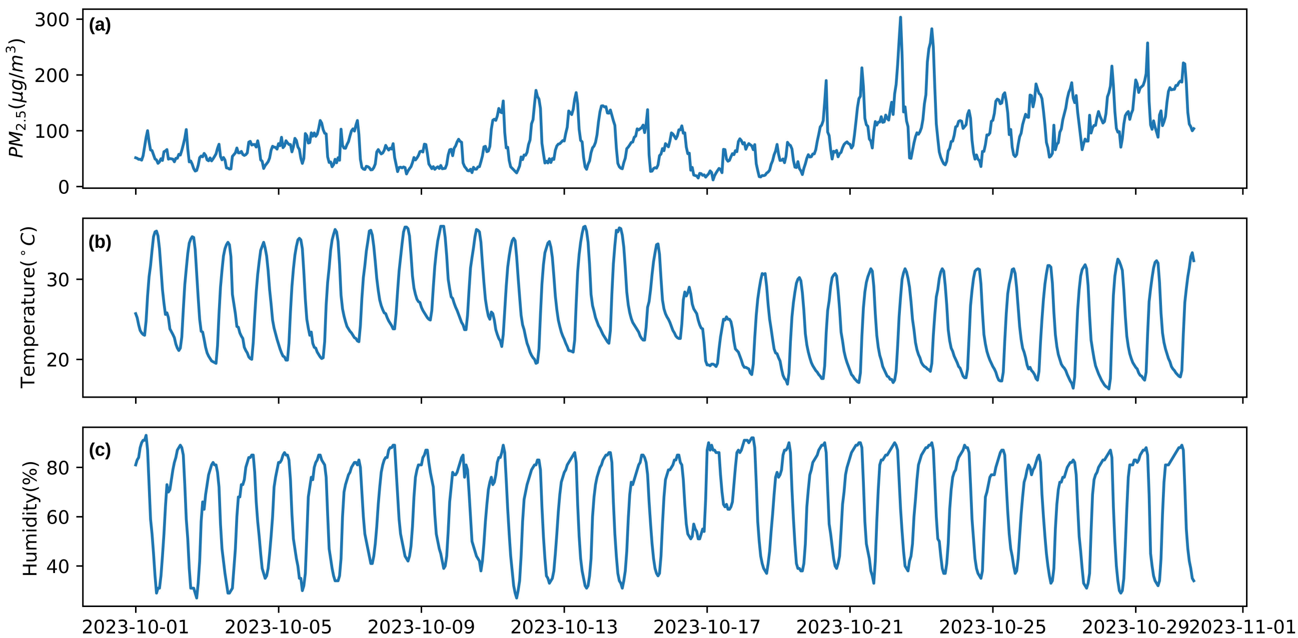

Figure 2. Time-series variation of (a) $PM_{2.5}$ (BAM), (b) temperature, and (c) humidity. Lower $PM_{2.5}$ levels are evident during the initial 16 days which can be attributed to higher temperatures, followed by higher $PM_{2.5}$ levels coinciding with lower temperatures, likely due to rain. The diurnal variation in humidity remained consistent, except on the 16th, 17th, and 18th of October, which saw rainfall.

and lower humidity. The diurnal variation ranged from 44.5 μg/m^3 to 253 μg/m^3, with an average of 107.35 μg/m^3. On a large majority of the days (83%), diurnal variation was found to be between 50 μg/m^3 and 150 μg/m^3.

3 Results and Discussion

Each LCS recorded data at 15 second resolution during the experiment, which was then aggregated into 5, 10, 15, 30, and 60 minutes intervals. For each interval, samples are taken from the midpoint of the corresponding group and averaged hourly. Additionally, hourly averages of the 15 second LCS data are also considered. This results in six hourly average datasets for each LCS unit based on different sampling intervals. These hourly averaged LCS datasets were grouped by sampling interval and compared to BAM measurement. The time-series plot of this data reveals significant overlap among the LCS datasets indicating high precision. To quantify this precision, standard deviation (SD) and coefficient of variation (CV) are calculated in accordance with the USEPA guidelines.

The SD is computed as:

$$\mathrm{SD} = \sqrt{\frac{1}{(NM-1)} \sum_{j=1}^{M} \sum_{d=1}^{N} (x_{dj} - \bar{x}_d)^2} \tag{1}$$

https://doi.org/10.5194/ar-2024-39
Preprint. Discussion started: 13 December 2024

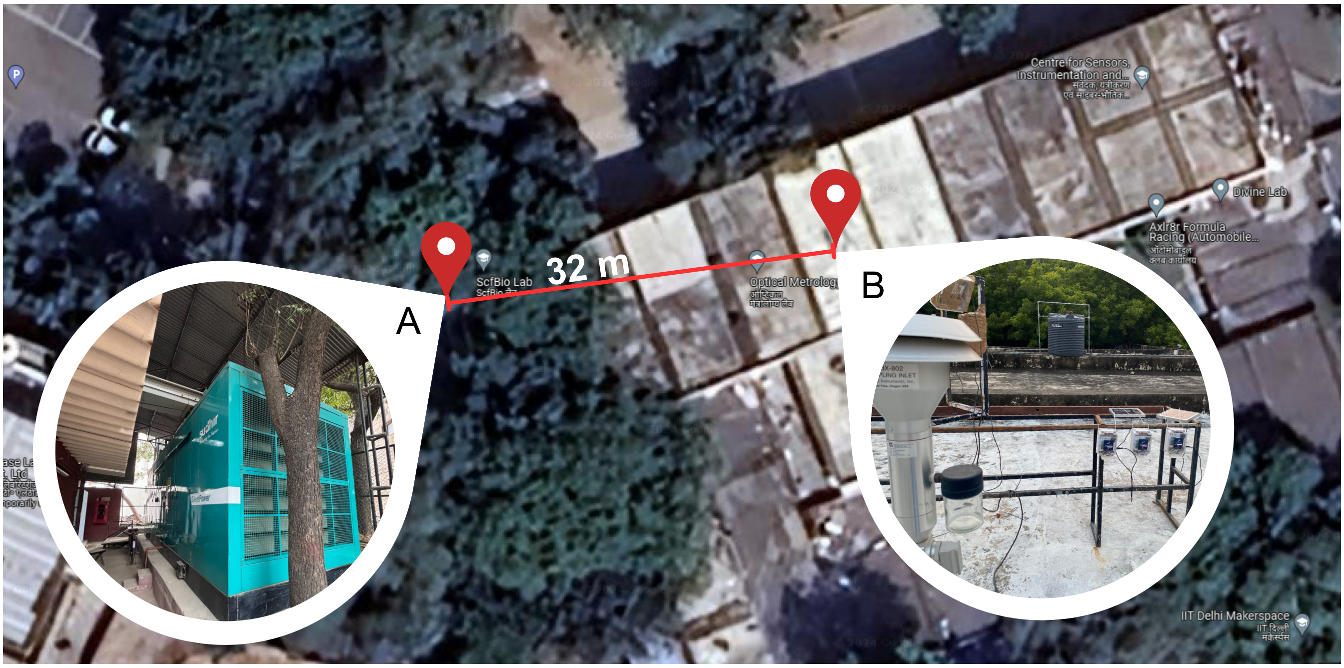

Figure 3. Location of study. The monitoring device was installed near a BAM on the rooftop of a building (B). Near the site there is a power backup building (A) located 32 m from B. Site A has three diesel generators.

where N is the number of 24-hour (daily) periods during which an LCS unit reported valid measurements, M is the number of LCS units, $\bar{x}_d$ is daily average LCS $PM_{2.5}$ concentration for the d^{th} day, and x_{dj} is daily average $PM_{2.5}$ concentration for d^{th} day and j^{th} LCS unit.

The daily average for the five LCS units was 89.56 μg/m^3, with a standard deviation of 3.92 μg/m^3 and a coefficient of variation of 4.38%, indicating high precision among the five LCS. Based on this, we employ only one LCS (S1) for the rest of the analysis, as repeating the analysis with other LCS would yield similar results.

3.1 Effect of LCS Sampling Interval on Linearity and Error

To assess the impact of LCS sampling interval on the correlation of the LCS data with BAM, we compute the coefficient of determination (R^2), slope (m), intercept (b), root mean square error (RMSE), and normalized root mean square error (NRMSE) (Duvall et al., 2021; Zimmerman, 2022). Scatter plots between different hourly averaged samples of S1 and reference BAM are shown in Figure 5, with error and linearity parameters indicated within each subplot. While it is commonly assumed that higher sampling rate leads to a better correlation with the reference BAM, from Figure 5 it is seen that differ-

https://doi.org/10.5194/ar-2024-39
Preprint. Discussion started: 13 December 2024

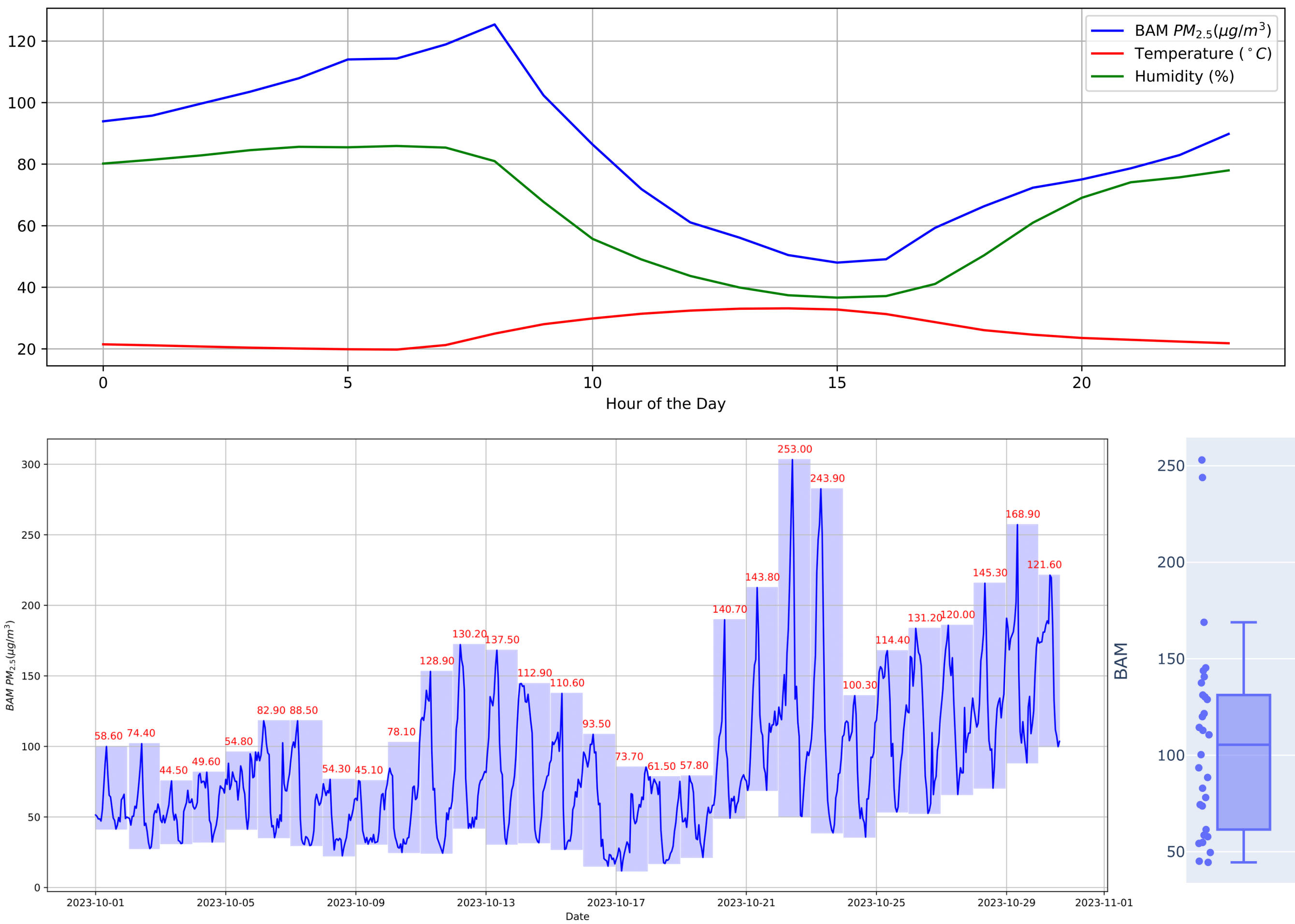

Figure 4. (a) Hourly averaged diurnal variations of $PM_{2.5}$ (BAM), temperature, and humidity levels. The x-axis denotes the hour of the day. $PM_{2.5}$ levels exhibit a direct correlation with humidity and an inverse relationship with temperature. Peak $PM_{2.5}$ levels are observed during morning hours with lower levels in the afternoon. (b) Time-series variation of $PM_{2.5}$ (BAM). Each day's diurnal variation is shown shaded in blue, with red text at the top indicating the range of diurnal variation for that day. (c) Box-plot showing the diurnal variation range for all days of the study.

https://doi.org/10.5194/ar-2024-39
Preprint. Discussion started: 13 December 2024

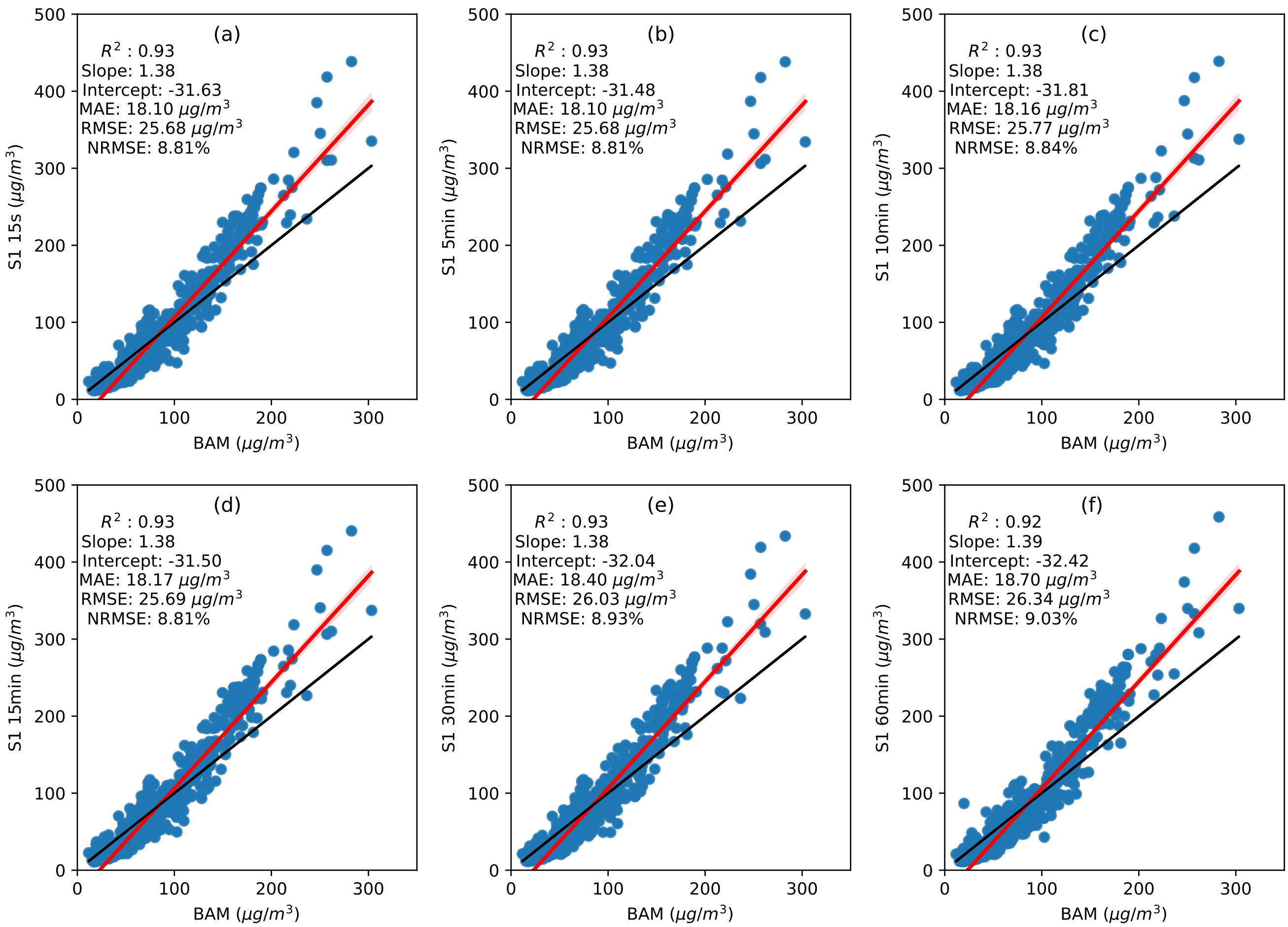

Figure 5. Scatter plots comparing LCS S1 and BAM hourly averaged data for different LCS sampling frequencies. Each subplot includes a regression line in red and a 1:1 ratio line in black. Additionally, linearity and error parameters are indicated within each subplot.

ent sampling intervals result in similar errors and other parameters. The reason behind similar results for different sampling intervals is averaging of the data and gradual variation in $PM_{2.5}$ levels.

3.2 Effect of LCS Sampling Interval on Hourly Average

An investigation into extreme cases is conducted using LCS data sampled at 15 second intervals. Hourly initial-final change in $PM_{2.5}$ concentrations was calculated, along with the hourly extremum difference within each hour. Hourly initial-final change represents the difference between the first and the last samples taken within an hour and hourly extremum is the difference between the highest and lowest values recorded within the hour. Hourly extremum is especially helpful in detecting short lived plume events. During our study, minimum hourly initial-final change was observed at 2023-10-08 14:00:00 (0.03 $\mu g/m^3$),

https://doi.org/10.5194/ar-2024-39
Preprint. Discussion started: 13 December 2024

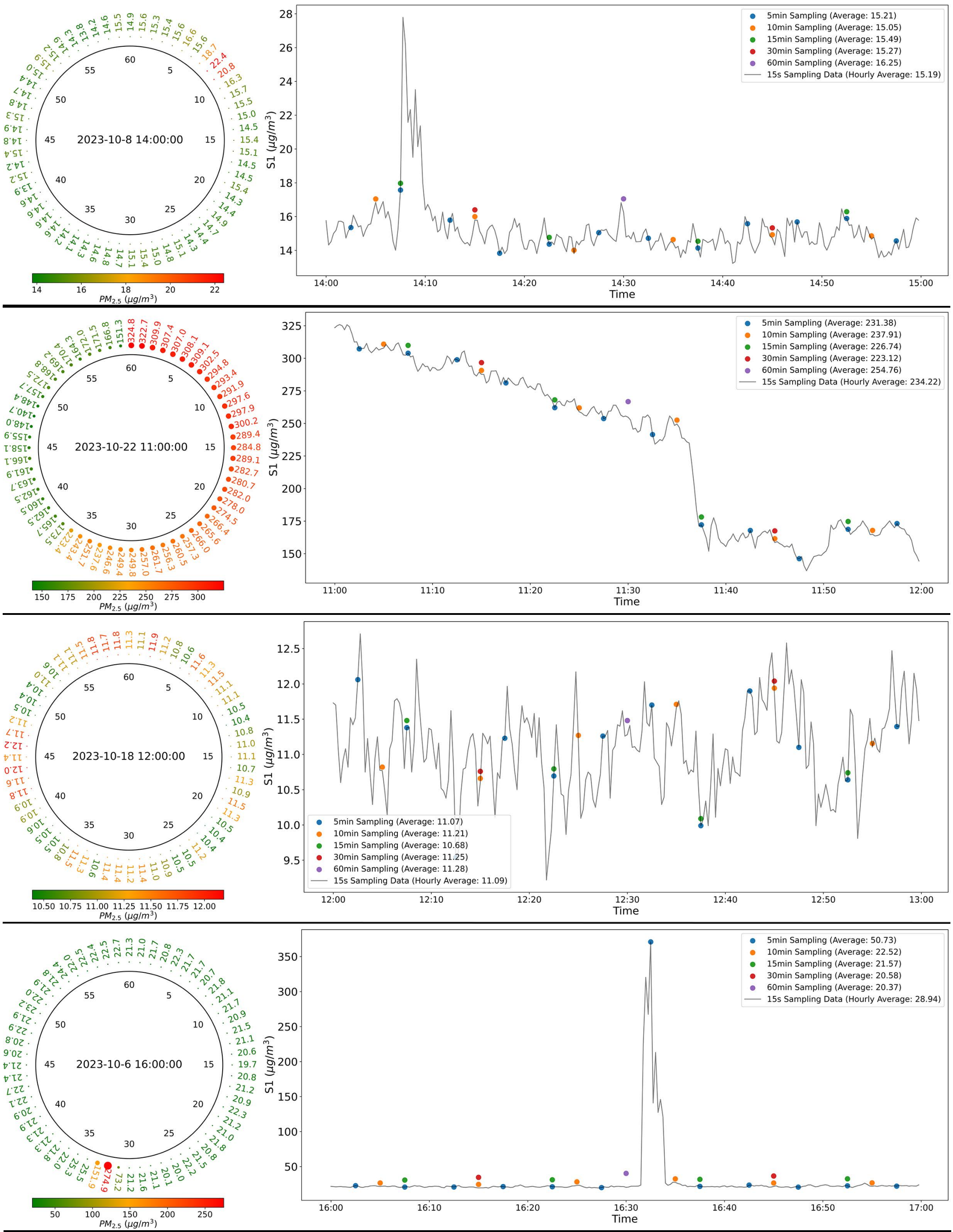

Figure 6. The clock within each subplot shows $PM_{2.5}$ variation for a particular hour, indicated at the center of the clock. The minute averaged $PM_{2.5}$ data is shown around the circumference of the clock. The time series plot within each subplot shows the 15 second data for the same hour, with different colored dots representing samples for different sampling intervals. For instance, green dots represent data over every 15 minutes, resulting in four data points per hour. The four subplots represent different one hour periods with extreme cases: (a) shows the hour with minimum change in $PM_{2.5}$ levels between the first and last sample, (b) shows the hour with highest variation in $PM_{2.5}$ levels between the first and last sample, (c) shows the hour with minimum variation in $PM_{2.5}$ levels across all samples collected during that hour, and (d) shows the hour with maximum variation in $PM_{2.5}$ levels across all samples collected during that hour.

https://doi.org/10.5194/ar-2024-39
Preprint. Discussion started: 13 December 2024

while the maximum hourly initial-final change was observed at 2023-10-22 11:00:00 (179.035 μg/m^3)(refer Figure 6(a),(b)). Additionally, the minimum hourly extremum was recorded at 2023-10-18 12:00:00 (3.49 μg/m^3), while the maximum hourly extremum was observed at 2023-10-06 16:00:00 (351.69 μg/m^3) (refer Figure 6(c),(d)). Considering the hourly average of these extreme events shown in Figure 6 indicates that despite these being extreme events, the hourly averages for different sampling intervals remain consistent. This analysis shows that varying the sampling frequency does not significantly impact the hourly average.

3.3 Plume Event Detection

Plume events, characterized by short duration spikes in particulate matter concentration, can arise from various sources such as vehicular traffic, cooking, waste burning, and backup power generators. These events are crucial to measure as they often go undetected, when data is recorded at lower sampling rates, but can have significant implications. In this study, the potential applications of high-frequency PM data are examined based on the observation that sampling frequency has minimal impact on hourly averages. Data from LCS S1 collected at 15 second intervals, along with the corresponding hourly averages and the reference BAM hourly average data are analyzed to understand their differences (refer Figure 7). Numerous spikes are observed in the 15 second data that are not seen in the hourly averages. An example of such a spike is shown in Figure 6(d) and Figure 7 for the datetime 2023-10-6 16:00:00. These brief plume events, lasting less than 5 minutes, are not detected in most sampling intervals and show minimal or no impact on the hourly averaged data. Such events occurred on 13 out of 30 days during our experiment. In our investigation, we identified a backup power generator located approximately 30 m from the experiment site as a significant source for these plume events. Emissions from diesel generators, particularly during startup and operation, are well-documented in the literature (Zhu et al., 2009). Analysis of the generator's operational log revealed that its use during power outages was responsible for 61% of the observed spike events. The generator was operated for very short periods, producing plumes upon startup. Additional plume events could potentially be attributed to cleaning activities and other short-lived emission sources in the vicinity.

4 Conclusion

This study, conducted over a period of one month, where LCS were collocated with a reference BAM has provided several important insights into LCS performance. The LCS and reference BAM exhibit consistent trends, along with a correlation between humidity and $PM_{2.5}$ levels. Higher $PM_{2.5}$ levels were observed in the morning hours due to higher humidity and vehicular activity, while lower $PM_{2.5}$ levels were recorded in the afternoon as the temperatures rise. The SPS30 LCS units demonstrated high precision, with a CV of 4.38%. While previous studies have established the health risks associated with short and long-term $PM_{2.5}$ exposure, in this work we investigated the impact of sampling frequency on the ability to detect short-lived plume events. We showed that while lower sampling frequencies are adequate for monitoring long-term trends, higher frequency data is necessary to capture short-lived plume events. In addition, our analysis revealed that varying the sampling frequency had minimal impact on the measurement accuracy, however only high frequency sampling (15 second sampling interval) was effec-

https://doi.org/10.5194/ar-2024-39
Preprint. Discussion started: 13 December 2024

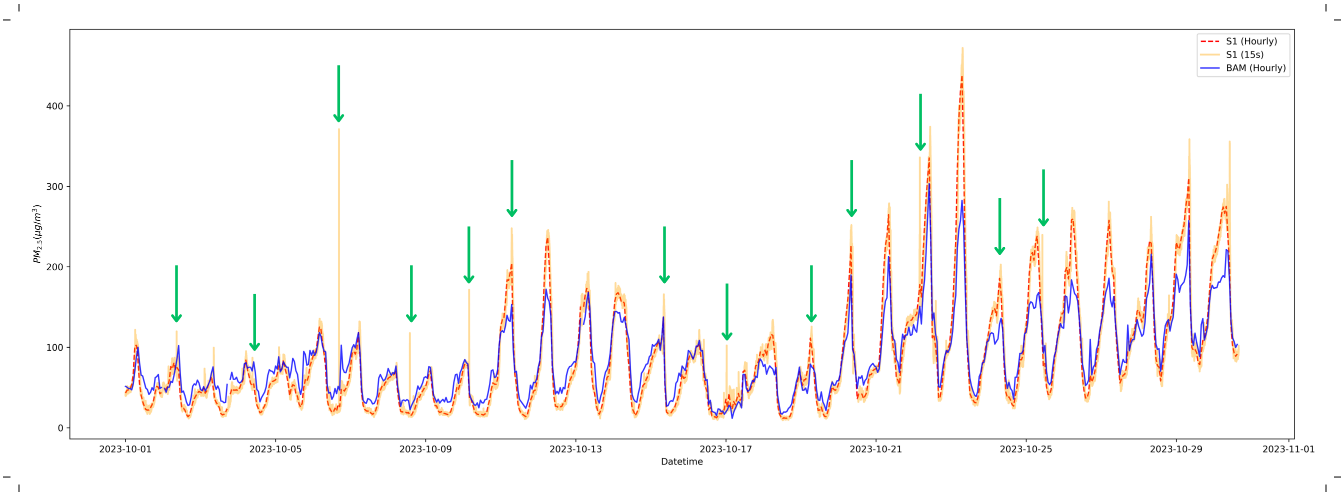

Figure 7. Time-series plot of 15 second and hourly averaged $PM_{2.5}$ data from the LCS S1 and BAM. The hourly averages of BAM and S1 exhibit a consistent trend, similar to the 15 second data from S1. However, the 15 second data of S1 reveals additional spikes (indicated by green arrows), corresponding to plume events. These transient events are not captured by the hourly averaged data from S1 or the hourly data from BAM.

tive in capturing the transient plume events. Although short-term health assessment was not within the scope of this study, the findings offer valuable guidance for future research, particularly in deciding the sampling frequency for different monitoring objectives. Additionally, our study suggests that for deployments based on low-cost, standalone PM monitors which need to be solar-powered or battery-operated, if the goal is to capture overall pollution trend rather than short-lived events, lower sampling frequencies provide similar long-term averages as high-frequency data. This enables the PM monitors to minimize their energy consumption and extend their operational life thus allowing for their long-term deployment in remote or resource-constrained areas. This work underscores the importance of customized sampling strategy while validating the use of LCS for capturing long-term trends as well as short-term exposure events in air quality monitoring.

Code and data availability. The raw data is available at https://zenodo.org/records/14230696 (Kumar et al.). The code can be provided upon request from the author.

Author contributions. G.K. carried out the data analysis and prepared first draft of the manuscript. P.K.D. developed the sensing monitor and carried out the experiments. J.D. and S.S. initiated this research, contributed to the design and planning of the experiments, helped with statistical analyses, provided feedback. All co-authors contributed to revising the manuscript.

https://doi.org/10.5194/ar-2024-39
Preprint. Discussion started: 13 December 2024

Competing interests. The authors declare no competing interest.

References

Xiaoting Liu, Rohan Jayaratne, Phong Thai, Tara Kuhn, Isak Zing, Bryce Christensen, Riki Lamont, Matthew Dunbabin, Sicong Zhu, Jian Gao, David Wainwright, Donald Neale, Ruby Kan, John Kirkwood, and Lidia Morawska. Low-cost sensors as an alternative for long-term air quality monitoring. *Environ. Res.*, 185(109438):109438, 2020.

Michael R Giordano, Carl Malings, Spyros N Pandis, Albert A Presto, V F McNeill, Daniel M Westervelt, Matthias Beekmann, and R Subramanian. From low-cost sensors to high-quality data: A summary of challenges and best practices for effectively calibrating low-cost particulate matter mass sensors. *J. Aerosol Sci.*, 158(105833):105833, 2021.

Wan Jiao, Gayle Hagler, Ronald Williams, Robert Sharpe, Ryan Brown, Daniel Garver, Robert Judge, Motria Caudill, Joshua Rickard, Michael Davis, Lewis Weinstock, Susan Zimmer-Dauphinee, and Ken Buckley. Community air sensor network (CAIRSENSE) project: evaluation of low-cost sensor performance in a suburban environment in the southeastern united states. *Atmos. Meas. Tech.*, 9(11):5281–5292, 2016.

Tongshu Zheng, Michael H Bergin, Ronak Sutaria, Sachchida N Tripathi, Robert Caldow, and David E Carlson. Gaussian process regression model for dynamically calibrating and surveilling a wireless low-cost particulate matter sensor network in delhi. *Atmos. Meas. Tech.*, 12 (9):5161–5181, 2019.

Wei Ying Yi, Kin Ming Lo, Terrence Mak, Kwong Sak Leung, Yee Leung, and Mei Ling Meng. A survey of wireless sensor network based air pollution monitoring systems. *Sensors (Basel)*, 15(12):31392–31427, 2015.

Shih-Chun Candice Lung, Wen-Cheng Vincent Wang, Tzu-Yao Julia Wen, Chun-Hu Liu, and Shu-Chuan Hu. A versatile low-cost sensing device for assessing PM2.5 spatiotemporal variation and quantifying source contribution. *Sci. Total Environ.*, 716(137145):137145, 2020.

Payali Das, Sushmita Ghosh, Shouri Chatterjee, and Swades De. A low cost outdoor air pollution monitoring device with power controlled built-in PM sensor. *IEEE Sens. J.*, 22(13):13682–13695, 2022.

Sunil Gulia, Poonam Prasad, S K Goyal, and Rakesh Kumar. Sensor-based wireless air quality monitoring network (SWAQMN) - a smart tool for urban air quality management. *Atmos. Pollut. Res.*, 11(9):1588–1597, 2020.

Grant R McKercher, Jennifer A Salmond, and Jennifer K Vanos. Characteristics and applications of small, portable gaseous air pollution monitors. *Environ. Pollut.*, 223:102–110, 2017.

Carolin Helbig, Maximilian Ueberham, Anna Maria Becker, Heike Marquart, and Uwe Schlink. Wearable sensors for human environmental exposure in urban settings. *Curr. Pollut. Rep.*, 7(3):417–433, 2021.

Yuzhi Xi, David B Richardson, Abhijit V Kshirsagar, Timothy J Wade, Jennifer E Flythe, Eric A Whitsel, Geoffrey C Peterson, Lauren H Wyatt, and Ana G Rappold. Effects of short-term ambient PM2.5 exposure on cardiovascular disease incidence and mortality among U.S. hemodialysis patients: a retrospective cohort study. *Environ. Health*, 21(1):33, 2022.

Sakshi Jain, Albert A Presto, and Naomi Zimmerman. Spatial modeling of daily PM2.5, NO2, and CO concentrations measured by a low-cost sensor network: Comparison of linear, machine learning, and hybrid land use models. *Environ. Sci. Technol.*, 55(13):8631–8641, 2021.

Kirsten A Koehler and Thomas M Peters. New methods for personal exposure monitoring for airborne particles. *Curr. Environ. Health Rep.*, 2(4):399–411, 2015.

R Duvall, A Clements, G Hagler, A Kamal, Vasu Kilaru, L Goodman, S Frederick, K Barkjohn, I VonWald, D Greene, et al. Performance testing protocols, metrics, and target values for fine particulate matter air sensors: use in ambient, outdoor, fixed site, non-regulatory supplemental and informational monitoring applications. *US EPA Office of Research and Development*, 2021.

Carl Malings. Integrating low-cost sensor systems and networks to enhance air quality applications. In *India Clean Air Summit (ICAS) 2024*, 2024.

Sensirion. Datasheet SPS30. Technical report, Sensirion AG, 2024. URL https://sensirion.com/media/documents/8600FF88/64A3B8D6/Sensirion_PM_Sensors_Datasheet_SPS30.pdf. Accessed: 2024-10-30.

Plantower. PMS7003 Series Data Manual. Technical report, Plantower, 2024. URL https://download.kamami.pl/p564008-PMS7003%20series%20data%20manua_English_V2.5.pdf. Accessed: 2024-10-30.

Honeywell. HPM Series Particulate Matter Sensors. Technical report, Honeywell International Inc., 2024. URL https://prod-edam.honeywell.com/content/dam/honeywell-edam/sps/siot/en-us/products/sensors/particulate-matter-sensors-hpm-series/documents/sps-siot-particulate-hpm-series-datasheet-32322550-ciid-165855.pdf. Accessed: 2024-10-30.

Kamaljeet Kaur and Kerry E Kelly. Laboratory evaluation of the alphasense OPC-N3, and the plantower PMS5003 and PMS6003 sensors. *J. Aerosol Sci.*, 171(106181):106181, 2023.

Marc Fadel, Frédéric Ledoux, Marianne Seigneur, Konstantina Oikonomou, Jean Sciare, Dominique Courcot, and Charbel Afif. Chemical profiles of PM2.5 emitted from various anthropogenic sources of the eastern mediterranean: Cooking, wood burning, and diesel generators. *Environ. Res.*, 211(113032):113032, 2022.

Helmut Greim. Diesel engine emissions: are they no longer tolerable? *Arch. Toxicol.*, 93(9):2483–2490, 2019.

Elisabeth A Gilmore, Lester B Lave, and Peter J Adams. The costs, air quality, and human health effects of meeting peak electricity demand with installed backup generators. *Environ. Sci. Technol.*, 40(22):6887–6893, 2006.

Kai Zhang and Stuart Batterman. Air pollution and health risks due to vehicle traffic. *Sci. Total Environ.*, 450-451:307–316, 2013.

Frederick W Lipfert and Ronald E Wyzga. On exposure and response relationships for health effects associated with exposure to vehicular traffic. *J. Expo. Sci. Environ. Epidemiol.*, 18(6):588–599, 2008.

Mydzung T Chu, Sara E Gillooly, Jonathan I Levy, Jose Vallarino, Lacy N Reyna, Jose Guillermo Cedeño Laurent, Brent A Coull, and Gary Adamkiewicz. Real-time indoor PM2.5 monitoring in an urban cohort: Implications for exposure disparities and source control. *Environ. Res.*, 193(110561):110561, 2021.

Jianbang Xiang, Jiayuan Hao, Elena Austin, Jeff Shirai, and Edmund Seto. Residential cooking-related PM2.5: Spatial-temporal variations under various intervention scenarios. *Build. Environ.*, 201(108002):108002, 2021.

Deepti Sharma and Suresh Jain. Impact of intervention of biomass cookstove technologies and kitchen characteristics on indoor air quality and human exposure in rural settings of india. *Environ. Int.*, 123:240–255, 2019.

Kalpana Balakrishnan, Sankar Sambandam, Padmavathi Ramaswamy, Sumi Mehta, and Kirk R Smith. Exposure assessment for respirable particulates associated with household fuel use in rural districts of andhra pradesh, india. *J. Expo. Anal. Environ. Epidemiol.*, 14 Suppl 1 (S1):S14–25, 2004.

Christine Wiedinmyer, Robert J Yokelson, and Brian K Gullett. Global emissions of trace gases, particulate matter, and hazardous air pollutants from open burning of domestic waste. *Environ. Sci. Technol.*, 48(16):9523–9530, 2014.

Kanchan Kumari, Sunil Kumar, Vineel Rajagopal, Ankur Khare, and Rakesh Kumar. Emission from open burning of municipal solid waste in india. *Environ. Technol.*, 40(17):2201–2214, 2019.

S Salvi, A Blomberg, B Rudell, F Kelly, T Sandström, S T Holgate, and A Frew. Acute inflammatory responses in the airways and peripheral blood after short-term exposure to diesel exhaust in healthy human volunteers. *Am. J. Respir. Crit. Care Med.*, 159(3):702–709, 1999.

Henry Gong, Jr, William S Linn, Constantinos Sioutas, Sheryl L Terrell, Kenneth W Clark, Karen R Anderson, and Lester L Terrell. Controlled exposures of healthy and asthmatic volunteers to concentrated ambient fine particles in los angeles. *Inhal. Toxicol.*, 15(4):305–325, 2003.

C Arden Pope, 3rd and Douglas W Dockery. Health effects of fine particulate air pollution: lines that connect. *J. Air Waste Manag. Assoc.*, 56(6):709–742, 2006.

Francesca Borghi, Giacomo Fanti, Andrea Cattaneo, Davide Campagnolo, Sabrina Rovelli, Marta Keller, Andrea Spinazzè, and Domenico Maria Cavallo. Estimation of the inhaled dose of airborne pollutants during commuting: Case study and application for the general population. *Int. J. Environ. Res. Public Health*, 17(17):6066, 2020.

Francesca Borghi, Andrea Spinazzè, Simone Mandaglio, Giacomo Fanti, Davide Campagnolo, Sabrina Rovelli, Marta Keller, Andrea Cattaneo, and Domenico Maria Cavallo. Estimation of the inhaled dose of pollutants in different micro-environments: A systematic review of the literature. *Toxics*, 9(6):140, 2021.

Jessica Tryner, John Mehaffy, Daniel Miller-Lionberg, and John Volckens. Effects of aerosol type and simulated aging on performance of low-cost PM sensors. *J. Aerosol Sci.*, 150(105654):105654, 2020.

F A Roberts, Kathryn Van Valkinburgh, Austin Green, Christopher J Post, Elena A Mikhailova, Sarah Commodore, John L Pearce, and Andrew R Metcalf. Evaluation of a new low-cost particle sensor as an internet-of-things device for outdoor air quality monitoring. *J. Air Waste Manag. Assoc.*, 72(11):1219–1230, 2022.

Low-power operation. https://sensirion.com/media/documents/188A2C3C/6166F165/Sensirion_Particulate_Matter_AppNotes_SPS30_Low_Power_Operation_D1.pdf.

Air quality sensor summary reports. http://www.aqmd.gov/aq-spec/evaluations/summary-pm.

Tca9548a low-voltage 8-channel i2c switch. https://www.ti.com/lit/ds/symlink/tca9548a.pdf?ts=1710275256813&ref_url=https%253A%252F%252Fwww.google.com%252F.

Naomi Zimmerman. Tutorial: Guidelines for implementing low-cost sensor networks for aerosol monitoring. *J. Aerosol Sci.*, 159(105872):105872, 2022.

Dongzi Zhu, Nicholas J Nussbaum, Hampden D Kuhns, M-C Oliver Chang, David Sodeman, Sebastian Uppapalli, Hans Moosmüller, Judith C Chow, and John G Watson. In-Plume emission test stand 2: emission factors for 10- to 100-kw U.S. military generators. *J. Air Waste Manag. Assoc.*, 59(12):1446–1457, 2009.

Gulshan Kumar, Prasannaa Kumar D., Raj Saran, Jay Dhariwal, and Seshan Srirangarajan. Impact of sampling frequency on low-cost pm sensor performance dataset. https://zenodo.org/records/14230696.